-Journal of Applied Chemical Research, 8, 3, 63-80 (2014)

Journal of Applied Chemical Research
www.jacr.kiau.ac.ir

Synthesis and Swelling Behavior of Gelatin-Based Hydrogel Nanocomposites

Gholam Bagheri Marandi*, Ghazal Beheshti Rouzbahani, Mehran Kurdtabar

Department of Chemistry, College of Basic Sciences, Karaj Branch, Islamic Azad University, Alborz, Iran

Received 17 Feb. 2014; Final version received 19 May 2014

Abstract

In this work, a series of hydrogel nanocomposites were prepared by grafting acrylic acid and acrylamide on gelatin in the presence of Na-montmorillonite (Na-MMT) nanoparticles. The characterizations of hydrogel nanocomposites were examined by swelling experiments, Fourier transform infrared (FT-IR) spectroscopy, X-Ray diffraction (XRD) patterns and thermogravimetric analysis (TGA). Scanning electron microscopy (SEM) was used to study the morphology of the samples. Under the optimized conditions the maximum capacity of swelling in de-ionized water was found to be 375 g/g. In spite of the sensitivity of the hydrogel absorbency to environmental pH, these hydrogel nanocomposites interestingly do not show remarkable changes in wide range of pH (from pH 4 to 10).

Keywords*: *Hydrogel, Gelatin, Nanocomposite, Acrylic acid, Acryl amide.

Introduction

Superabsorbent hydrogels are a type of loosely crosslinked hydrophilic polymers that can swell, absorb and preserve a large volume of water or other biological fluids in their three dimensional networks [1, 2]. Superabsorbents have great advantages over traditional water-absorbing materials such as cotton, pulp, and sponges. In the recent two decades, there has been considerable interest in these water-swellable polymers. Due to their excellent response to changing environment conditions such as temperature [3], pH [4], and solvent composition [5], superabsorbent hydrogels have been attracting in many industrial and medical applications [6-9].

Natural-based superabsorbent hydrogels have attracted much attention in medical,

***Corresponding author:** Dr. Gholam Bagheri Marandi, Department of Chemistry, College of Basic Sciences, Karaj Branch, Islamic Azad University, Alborz, Iran. E-mail: Marandi@kiau.ac.ir.*

pharmaceutical, baby diapers, agriculture and horticulture because of their non-toxicity, biocompatibility and biodegradability. Graft-copolymerization of vinyl monomers onto natural-based polymers is an efficient method for the synthesis of these superabsorbents [10-12]. The higher production cost and lower gel strength of these hydrogels, however, restrict their application considerably in practice. To mitigate these limitations, cheaper inorganic compounds can be used. The introduction of inorganic fillers to a polymer matrix can sometimes increase its strength and stiffness [13, 14], and it will also promote the industrial application of the hydrogel composites [15, 16]. It has been reported that the type of dispersion of clay in composites determines the properties of polymer composites [17]. In addition to aggregated clay-polymer composites, intercalated and exfoliated clay-polymer composites can be produced using suitable methods [18]. It is required to use nano-scale clays to achieve intercalated or exfoliated composites [17, 19].

Gelatin is a high molecular weight polypeptide obtained by controlled hydrolysis of collagen. The most interesting feature of gelatin is that it can be used for the production of practical biocompatible materials [20]. Gelatin hydrogels can be used as biodegradable materials in the pharmaceutical and medical fields [21-24]. However, due to its weak mechanical strength, there is a limitation in application of gelatin to prepare hydrogels. In practical applications, the structure needs to be reinforced either through crosslinking or some filler materials. The introduction of clay minerals as a filler to the gelatin-based hydrogel structure causes a hydrogel composite and as well-known it is a useful method to increase both the mechanical strength and the thermal stability [25, 26].

In the present work, we report the synthesis of gelatin-based hydrogel nanocomposites by grafting acrylic acid (AA) and acrylamide (AAm) onto gelatin in the presence of Na-montmorillonite (Na-MMT) nanoparticles and N,N'-methylenebisacrylamide (MBA) as a crosslinker. The effect of clay content affecting the water absorbency of the hydrogel and swelling behavior in various salt solutions were also determined and additionally, the swelling of the hydrogels was measured in solutions with pH ranged 1-13. Interestingly, water absorbency slightly changes from pH 4 to 10. The time dependence of the water retention capacity (WRC) was also studied.

Experimental

Materials

Gelatin, AA, AAm, ammonium persulfate (APS), sodium hydroxide (all from Merck, Germany) and MBA (Fluka) were of analytical grade and use without further purification. Natural Na-MMT (sodium Cloisite) ($Si_4[Al_{1.67}Mg_{0.33}]O_{10}(OH)_2.nH_2O.Na_{0.33}$) as

a clay with cation exchange capacity of 92 meq/100 g of clay was provided by Southern Clay Products (USA). 90 vol% of its dry powder has particle size less than 13 μm, according to the manufacturer's information. De-ionized water was used for the hydrogel preparation and swelling measurements. All other chemicals were also of analytical grade.

Preparation of hydrogels

The amounts of the starting materials used for all the different series of the experiments are summarized in Table 1. As a general procedure, in a two-necked reactor equipped with a mechanical stirrer (Heidolph RZR 2021, three blade propeller type, 300 rpm), nanoclay was dissolved in 20 ml de-ionized water. After 15 min, a solution of 1 g gelatin in 20 mL de-ionized water added to the reactor. The reactor was immersed into the water bath at a desired temperature (70 °C). Then, the initiator solution (APS in 5 mL H_2O) was added to the mixture. After stirring for 5 min, 3.9 g of AA (80% neutralized in 5 mL H_2O), 0.71 g AAm (in 5 mL H_2O) and 0.05 g MBA (in 5 mL H_2O) were simultaneously added to the reaction mixture. After 60 min, the mixture was poured to excess non solvent ethanol (200 mL) and remained for 2 h to dewater. After ethanol was decanted, the product was cut into small pieces (diameter ~ 5 mm). Again 100 mL fresh ethanol was added and the hydrogel was remained for 24 h. Finally, the filtered hydrogel is dried in oven at 70 °C for 8 h. After grinding, the resulted powder was stored away from moisture, heat and light.

Table 1. Amount of reaction contents used in different sample preparations.

Sample	N0	N1	N2	N3
Na-MMT (g)	0	0.5	0.75	1
Gelatin (g)	1	1	1	1
AA (mol/L)	3.9	3.9	3.9	3.9
AAm (mol/L)	0.71	0.71	0.71	0.71
AA/ AAm weight ratio	5.5	5.5	5.5	5.5
MBA (mmol/L)	11	11	11	11
KPS (mmol/L)	8	8	8	8
ES (g/g)	283	295	316	268
Gel content (%)	54	54	56	59

Measurement of the Water Absorbency

A certain amount of each samples (0.05 ± 0.0001 g) with average particle sizes between 40-60 mesh (250-400 μm) were immersed in 250 mL distilled water for 2 h at room temperature to reach equilibrium swelling.

The equilibrium swelling (ES) was calculated according to the following equation:

$$ES(g/g) \quad \frac{W_s - W_d}{W_d} \qquad (1)$$

where W_s and W_d are the weights of the swollen and dry hydrogels, respectively.

Determination of Gel Content

To measure the gel content values, 0.05 g of superabsorbent nanocomposites dried powder was immersed in excess distilled water for 72 h. Then swollen samples were filtered, dewatered with ethanol and dried at 70 °C for 5 h. Dried samples reweighed and gel content (Gel %) was calculated by equation 2:

$$Gel\% \quad \frac{M_f}{M_i} \qquad (2)$$

where Mi and Mf are initial and final weight of sample, respectively. The results of determination of gel content have been presented in Table 1.

Swelling Kinetics

To study the absorbency rate of the hydrogels, certain amount of dry samples (0.05 g ± 0.0001) with different sizes were poured into numbers of weighed tea bags and immersed in 200 mL of distilled water for different contact times. At consecutive time intervals, the water absorbency of the samples was measured according to the above mentioned method.

Absorbency at Various pHs

Individual solutions with acidic and basic pH values were prepared by dilution of NaOH (pH 13.0) and HCl (pH 1.0) solutions to achieve pH ≥ 6.0 and pH < 6.0, respectively. The pH values were precisely checked by a pH-meter (Metrohm/620, accuracy ±0.1). Then, 0.05 g (± 0.0001) of the sample was used for the swelling measurements according to equation 1.

Swelling in Various Salt Solutions

According to the above method described for swelling measurement in distilled water, absorbency of the hydrogel nanocomposites measured in 0.15 M solution of LiCl, NaCl, KCl, $CaCl_2$, $MgCl_2$, $BaCl_2$, and $AlCl_3$. Also, swelling capacity of the samples was evaluated in different concentrations of NaCl, $CaCl_2$ and $AlCl_3$ salt solutions.

Swelling-Deswelling of the Hydrogel Nanocomposites in (H_2O-NaCl) and (NaCl-$CaCl_2$) Solutions

The deswelling of all samples was examined in 0.15 M solutions of NaCl. The swollen hydrogels in distilled water were immersed in 250 mL of this salt solution and at consecutive time periods, the absorbency was measured. Swelling-deswelling of the hydrogel nanocomposites was also investigated in 0.15 M solutions of NaCl-$CaCl_2$ salt systems. Swelling capacity of the hydrogels at each salt solution was measured according to equation

1 at consecutive time intervals (60 min).

Water Retention Capacity (WRC)

For measuring the water retention at constant temperature, the equilibrated hydrogels were drained in 100-mesh nylon bags for 2 h, and then the bags containing the gels were put into a oven through which passed a current of hot dry air at constant temperature. The weights of the bags were measured for every half an hour in order to investigate the relationship between their weights and the heating time.

Instrumental Analysis

The FTIR spectra were obtained in KBr pellets using a Perkin-Elmer Precisely-100 FTIR spectrophotometer (USA). X-ray diffraction patterns were gotten using a Philips X'Pert MPD X-ray diffractometer (Netherlands) with wavelength, λ=1.54Å (Cu-Kα), at a tube voltage of 40 kV, and tube current of 40 mA. The micrographs of optimized hydrogel nanocomposite were taken using scanning electron microscopy (SEM, Cambridge S-360), before SEM observation the sample was fixed on aluminum stub and coated with gold.

Results and discussion

Synthesis and Characterization

The mechanism for crosslinking graft copolymerization of co-monomers onto gelatin backbones in the presence of APS and MBA was shown in Scheme 1. At the first step, the thermal initiator (APS) which is sensitive to temperature will be decomposed in 70 °C and sulfate anion-radicals will be produced. The anion-radicals attack to the hydrogen of existing functional groups (i.e. CO_2H, SH, OH, and NH_2) in gelatin backbone to make the desired macroradicals. These radicals graft the AA, AAm and NaAA monomers to the gelatin. Finally the MBA and Na-MMT make the crosslinks between gelatin chains and network will be formed.

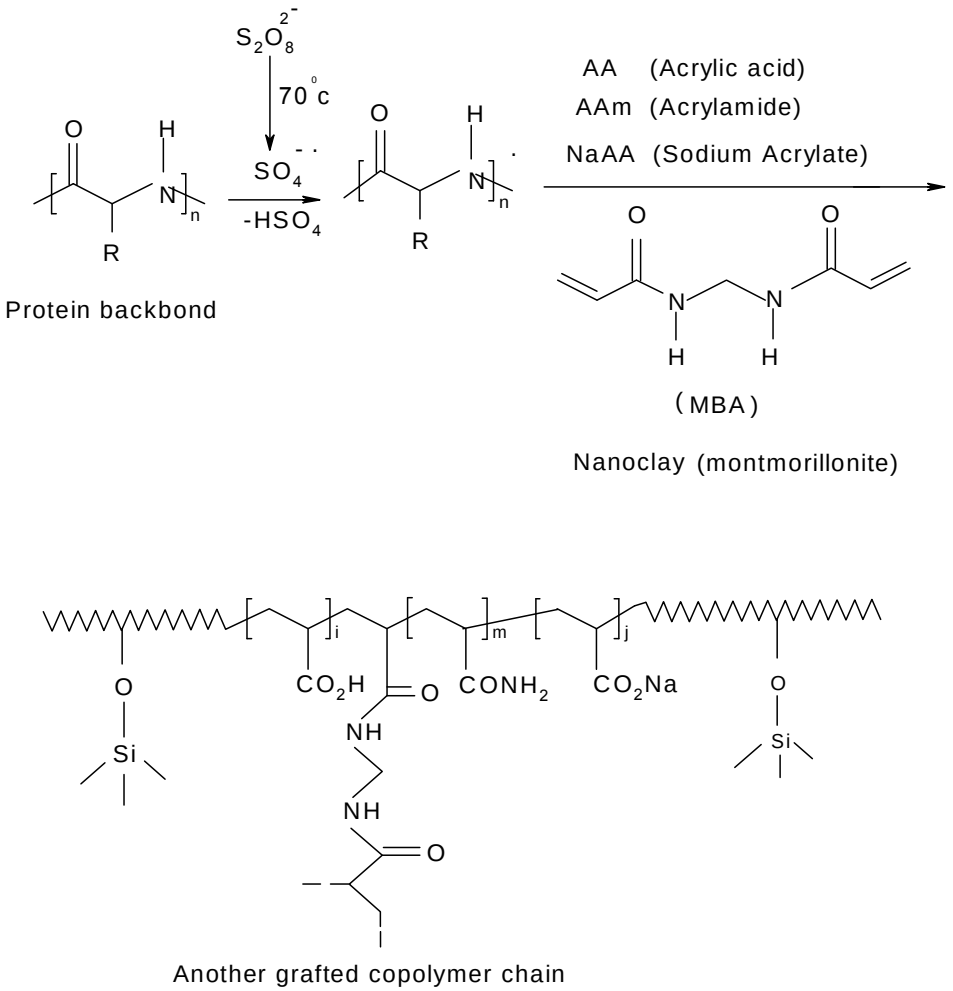

Scheme 1. Proposed mechanism for the synthesis of gelatin-*g*-poly(AA-co-AAm) hydrogel nanocomposite.

Figure 1 shows the FTIR spectra of Na-MMT (a), hydrogel nanocomposite (b) and clay-free hydrogel (c). In nanoclay (Na-MMT) spectra (a) the characteristic vibration bands of the nanoclay (-OH stretch from lattice hydroxyl, -OH stretch from free H_2O, -OH bending and Si-O stretch) are shown at 3634, 3447, 1638 and 1072 cm^{-1}, respectively. Also, the peak of 799 cm^{-1} is related to Al-O link. In Figure 1b, the broad band at 3435 cm^{-1} is due to stretching of hydroxyl groups of the gelatin. The band observed at 1675 cm^{-1} can be attributed to carbonyl stretching in carboxamide functional groups and also, two absorption peaks at 1565 and 1409 cm^{-1} were attributed to asymmetric and symmetric stretching of the COO^- groups, respectively. In addition, by compared with Figure 1a, the absorption peaks at 3634 and 3447 cm^{-1} (stretching of the OH groups on the nanoclay) disappeared after the reaction and also, peak at 1072 cm^{-1} (stretching of the Si-O group on the nanoclay) was weakened and shifted to 1048 cm^{-1} in nanocomposite. Therefore, it can suggest that the strong chemical interaction take place between the Si-O and –OH groups of the nanoclay

particles with functional groups of AA, AAm and NaAA during the graft polymerization reaction [23]. The FTIR of clay-free hydrogel was shown in Figure 1c. In the spectrum of graft copolymer, the peak at 1560 cm^{-1} is due to carbonyl asymmetric stretching in the carboxylate anion that is reconfirmed by another peak at 1412 cm^{-1}, which is related to a symmetric stretching mode of the carboxylate anion.

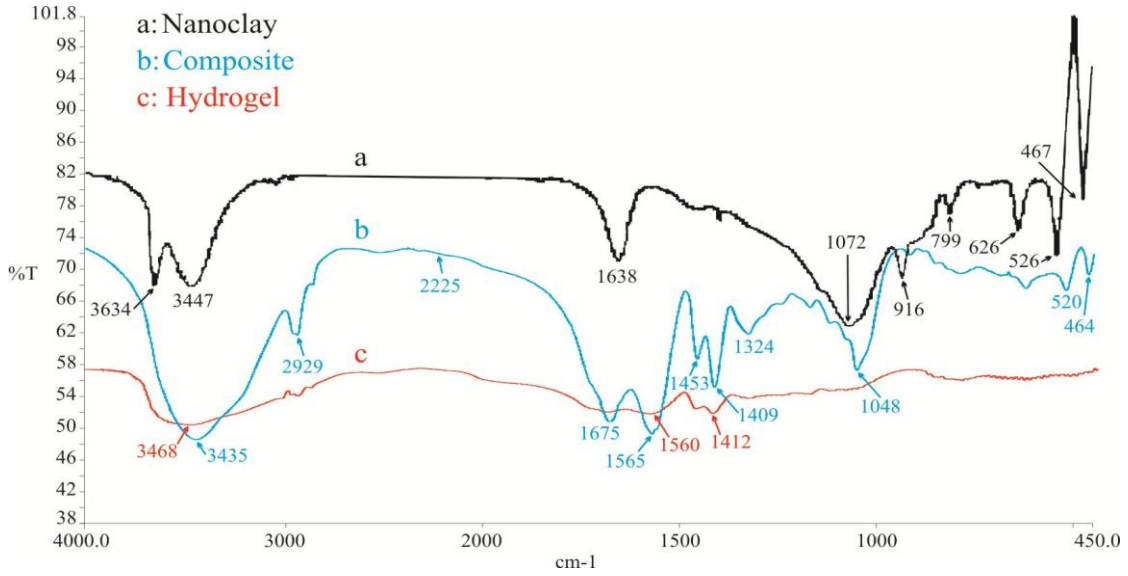

Figure 1. FT-IR spectra of Na-MMT (a), optimized nanocomposite (b) and hydrogel without nanoclay (c).

The microstructure morphologies are one of the most important properties that must be considered in hydrogels. The micrograph of optimized hydrogel nanocomposite has been depicted in Figure 2. As can be seen, the hydrogel nanocomposite represents an undulant and porous surface without agglomeration. These pores on the hydrogel surface are desired for water penetration into polymer network.

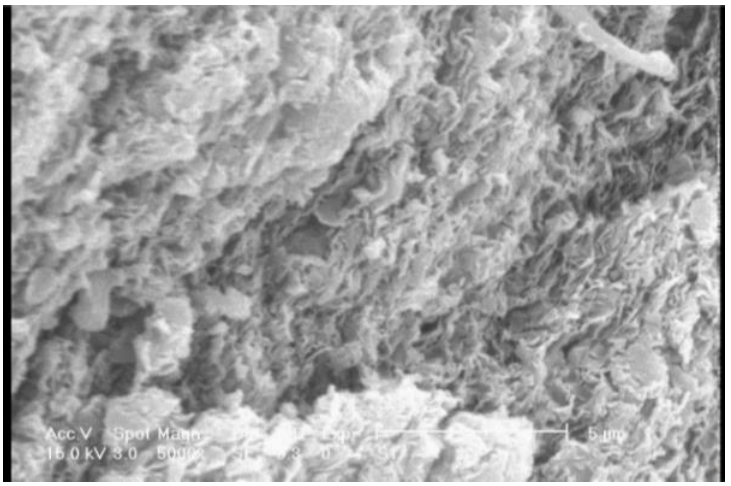

Figure 2. The SEM micrograph of optimized sample containing 0.75 g nanoclay with 5 µm scale bar.

The XRD profiles of Na-MMT and optimized content of Na-MMT containing sample were shown in Figure 3. The XRD pattern of Na-MMT with a peak at 2θ=7.6º was exhibited in Figure 3a. As shown in Figure 3b, no diffraction peak was observed in optimized sample. So, it can be concluded that the clay layers are completely exfoliated and uniformly dispersed in organic matrix.

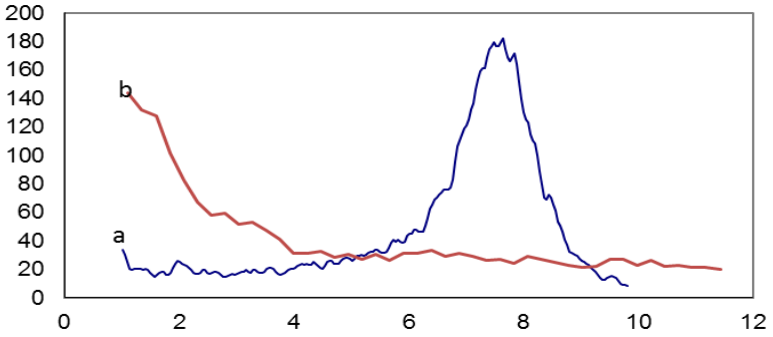

Figure 3. XRD patterns of nanoclay (a) and nanocomposite sample with 0.75 g nanoclay (b).

The thermogravimetric curves of the prepared hydrogels were depicted in Figure 4. In comparison to original decomposition temperature of 336 °C for the clay-free sample, maximum decomposition rate was shifted to 388 °C in the nanocomposite sample. As shown in Figure 4, it was found that the thermal stability of the nanocomposite was clearly improved.

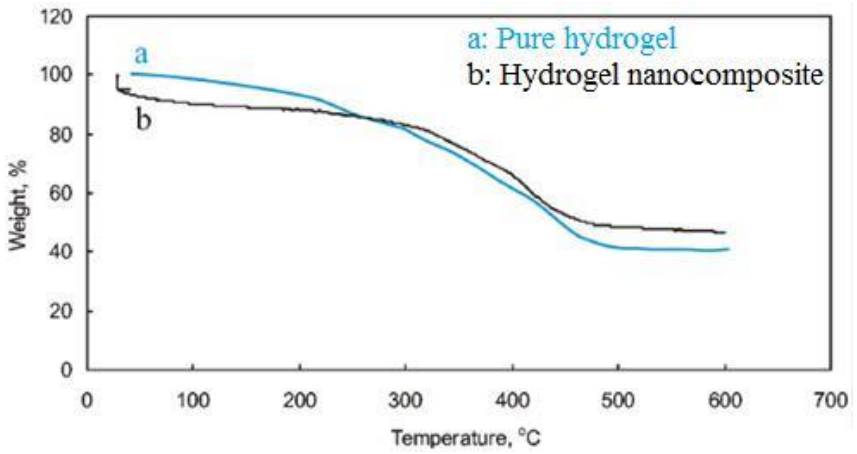

Figure 4. TGA thermograms of the pure hydrogel (a) and hydrogel nanocomposite with 0.75 g nanoclay (b).

The Effect of Na-MMT Content on Water Absorbency

In constant condition of other reactants, different amounts of Na-MMT (0.0-1.0 g) were used for hydrogel preparation. As can be seen in Figure 5, the water absorbency is substantially increased with increasing in the Na-MMT content and then it is decreased. The best absorption capacity and gel strength of the hydrogel were observed in 0.75 g

of Na-MMT. Increasing Na-MMT content increase hydrophilic groups, and because of the presence of different ions in clay structure move up the osmotic pressure of gel phase toward hydro phase. However excess content of Na-MMT leads to more crosslink points and as a result, elasticity of the polymeric chains decreases and polymeric network of hydrogel can not expand easily [28, 29].

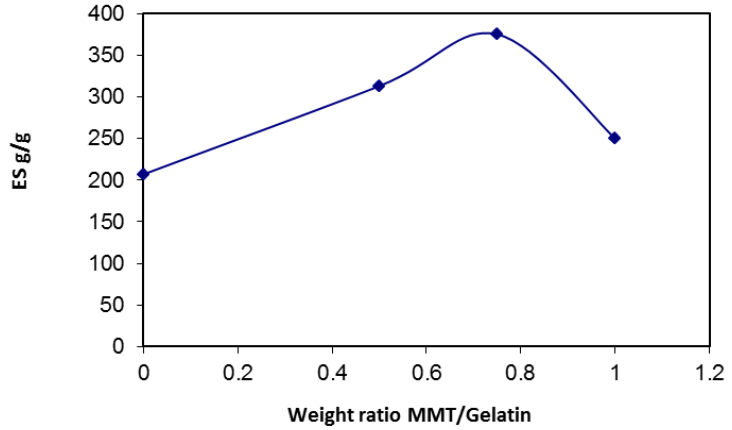

Figure 5. Effect of Na-MMT content on the water absorbency (Reaction conditions: AAm/ AA 0.186, MBA 1.61 mmol L^{-1}, APS 0.5 mmol L^{-1}, 70 ºC, neutralization percent 80 %, 60 min).

Swelling kinetics

In practical applications, not only is a higher swelling capacity required, but also a higher swelling rate is needed. The dynamic swelling behavior of hydrogels with different particle sizes (100-250, 250-400 and 400-550 µm) was determined and represented in Figures 6-8. The data can be fitted with a voigt base equation 3 [30]:

$$S_t \quad S_e(1 \quad e^{\frac{t}{W}}) \qquad (3)$$

where S_t (g/g) is swelling at time t, S_e is equilibrium swelling (power parameter, g/g), t is time (min) for swelling S_t, and τ (min) stands for the "rate parameter". To find the rate (τ) and power (S_e) parameters for hydrogels, the data obtained from swelling of the samples at consecutive time intervals were fitted into equation 3, using Origin 6.1 software. The results are summarized in Table 2. The values of swelling rate (SR, g/g.s) for the individual samples were determined from the following equation:

$$SR \quad \frac{S_{mW}}{W_{\min}} \qquad (4)$$

where $S_{m\tau}$ stands for swelling at the time related to the minimum rate parameter τ (s) obtained from hydrogels from a set of similar experiments (Table 2). The swelling of samples depend on the diffusion rate of water into their glassy matrix. As well-known with a lower particle size and a higher porosity, a higher rate of water uptake is observed in the hydrogels due to the increase in surface area

with decreasing particle size and the increase in capillary wetting with rising porosity [31, 32]. In the case of N2 sample, SR (g/g.s) for (400-550µm), (250-400 µm) and (100-250 µm) of particle size was 1.21, 1.55 and 2.28 while in the case of clay-free hydrogel these amounts were 0.85, 1.02 and 1.28, respectively. According to the results, it appears that the hydrophilic groups of nanoclay increase the rate of water absorbency in nanocomposite than clay-free hydrogel.

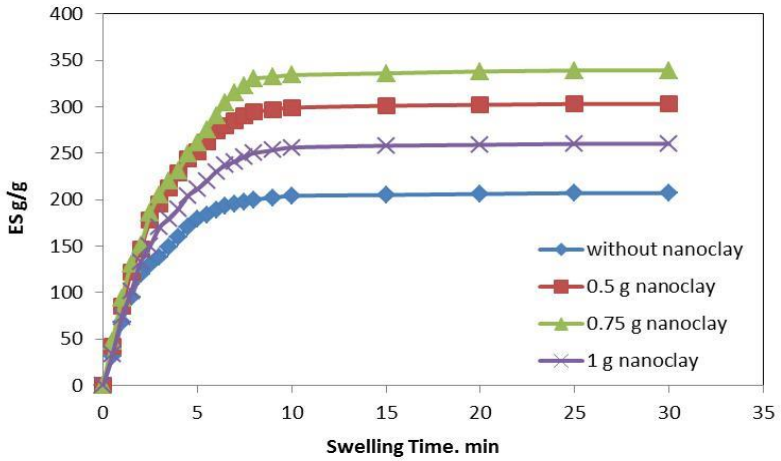

Figure 6. Swelling kinetic of the synthesized superabsorbents with 400-550 µm particle size.

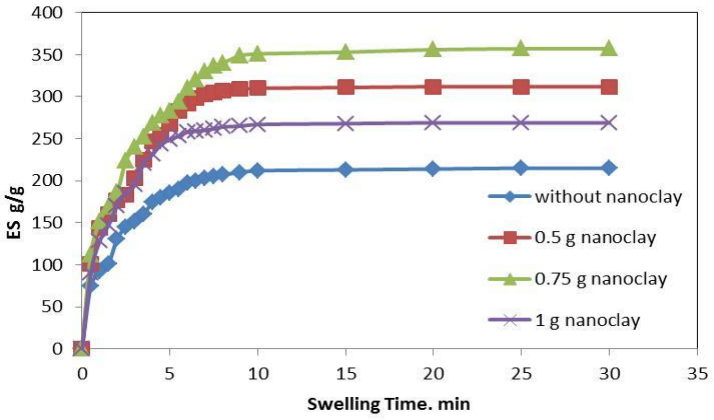

Figure 7. Swelling kinetic of the synthesized samples with 250-400 µm particle size.

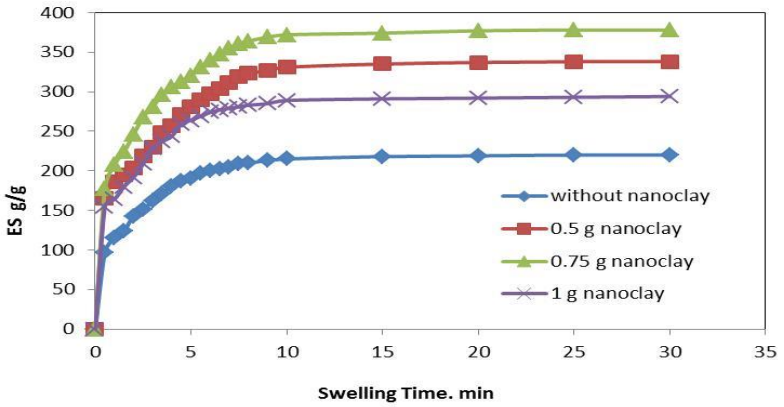

Figure 8. Swelling kinetic of the synthesized samples with 100-250 µm particle size.

Table 2. Values of ⅈ, S_e, $S_{Pⅈ}$, and SR for synthesized hydrogels with different particle size in distilled water.

Sample	Particle size (µm)	ⅈ (s)	S_e (g/g)	$S_{Pⅈ}$ (g/g)	SR (g/g.s)
N0		207.388	154.321	131.0942	0.84949
N1		307.7451	174.8252	180.4439	1.169276
N2	400-550	345.8735	198.8072	186.7248	1.209977
N3		262.7874	177.9359	152.3928	0.987505
N0		211.3422	130.3781	133.5938	1.024664
N1		312.3798	142.8571	186.9717	1.434073
N2	250-400	350.5935	151.7451	202.1156	1.550227
N3		266.9254	113.8952	181.9595	1.39563
N0		210.8702	104.2753	133.2954	1.278302
N1		320.7231	111.8568	194.4614	1.864884
N2	100-250	359.0019	96.43202	237.2491	2.275219
N3		280.6061	87.48906	195.3989	1.873876

Hydrogel Sensitivity to pH

Ionic hydrogels which could be cationic, anionic or amphoteric, have been reported to be very sensitive to changes in environmental pH [4, 33]. To evaluate this effect, the swelling of synthesized hydrogels was measured in different pH solutions ranged from 1.0 to 13.0. As shown in Figure 9, the absorbency of all samples increased sharply as the pH increased from 2 to 4 and drastically decreased in the

pH range of 11–13. In addition, the change in the water absorbency was slight from pH 4 to 11 which is probably because of the buffering effect of resulted hydrogels. In acidic media (pH=2-5), the swelling can be attributed principally to high repulsion between positively charged groups ($-NH_3^+$) in gelatin backbone of the hydrogel. Under very acidic conditions (pH<2), a screening effect of the counter ions, i.e. Cl^-, shield the charge of the ammonium cations in gelatin backbone and prevents efficient repulsion. As a result, absorbency is low. At higher pH values (pH=5-11), the swelling can be attributed principally to high repulsion between carboxylate groups ($–COO^-$) and increasing the osmotic pressure difference between polymeric network and external solution. In basic pH solutions (pH>11), charge screening effect caused, excess Na^+ shielded the carboxylate anions and prevented effective anion-anion repulsion consequently swelling capacity decreased. Similar swelling-pH dependencies have been reported in the case of other hydrogel systems [34, 35].

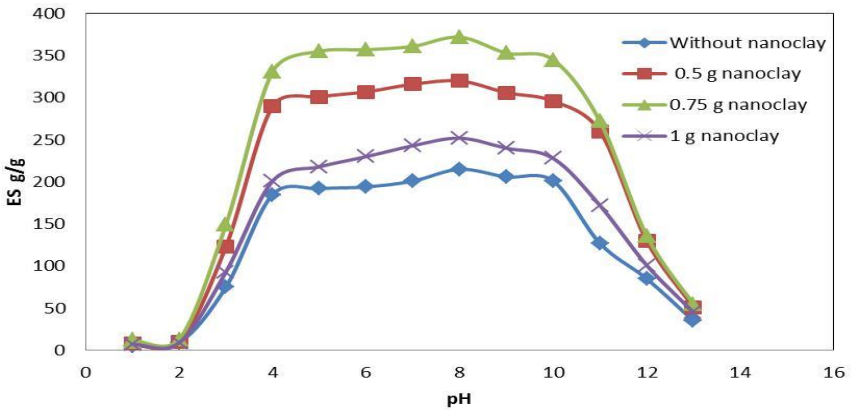

Figure 9. Swelling equilibrium of the superabsorbent hydrogels in solutions of various pHs.

Swelling Behavior in Various Salt Solution

Because the hydrogels can be considered as polyelectrolyte, they are sensitive to the ionic strength of the surrounding solution as well as their pH. As well-known the swelling of all ionic hydrogels would decrease significantly with increasing ionic strength of salt solutions. This could be attributed to the decrease in the osmotic pressure difference between the hydrogel and external salt solutions.

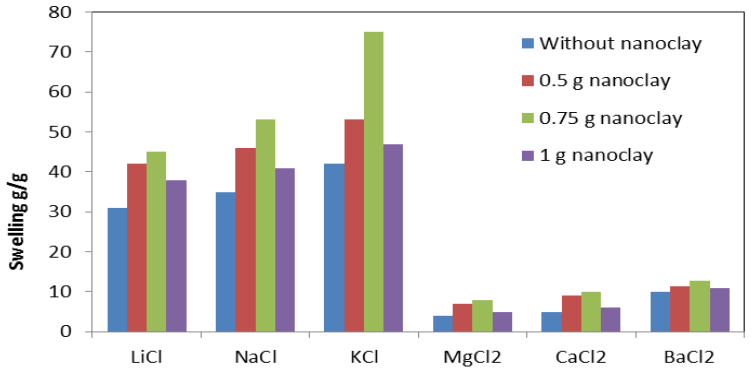

Figure 10. Swelling capacity of the superabsorbent hydrogels in different salt solutions.

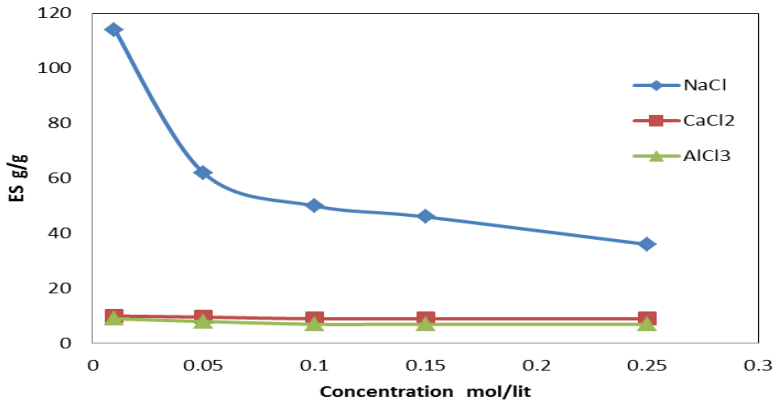

Figure 11. Swelling capacity of the superabsorbent hydrogel nanocomposites in different salt solutions. (Reaction conditions: AAm/ AA 0.186, Na-MMT/gelatin 0.5 g, MBA 1.61 mmol L^{-1}, APS 0.5 mmol L^{-1}, 70 ºC, neutralization percent 80%, 60 min).

Figures 10-13 show the effect of various salt solutions on water absorbency of the samples. According to these Figures, in the case of monovalent cations, decreased swelling ratio can be attributed to charge screening effect on anionic carboxylate groups. While in the case of divalent and trivalent cations, the networking effect causes an intensive decrease of water absorption capacity in addition to charge screening effect [36]. The effect of cation radius on swelling can also been observed from Figure 10.

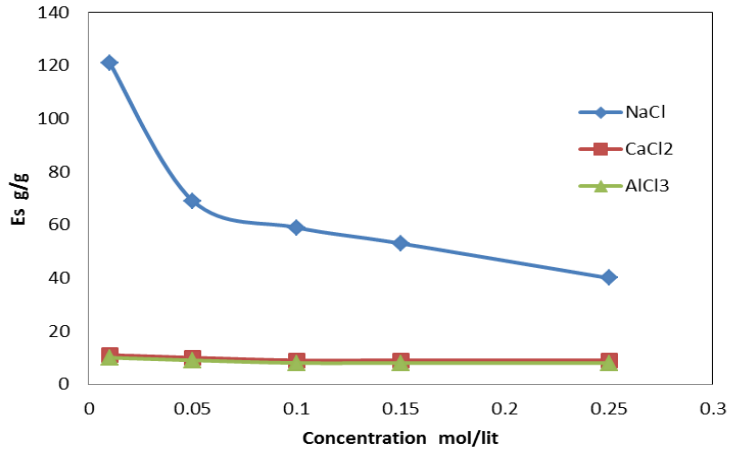

Figure 12. Swelling capacity of the superabsorbent hydrogel nanocomposites in different salt solutions. (Reaction conditions: AAm/ AA 0.186, Na-MMT/gelatin 0.75 g, MBA 1.61 mmol L^{-1}, APS 0.5 mmol L^{-1}, 70 ºC, neutralization percent 80%, 60 min).

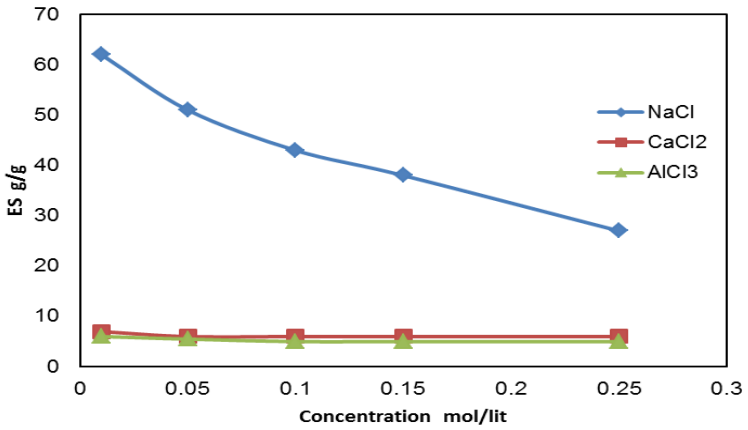

Figure 13. Swelling capacity of the superabsorbent hydrogel nanocomposites in different salt solutions. (Reaction conditions: AAm/ AA 0.186, Na-MMT/gelatin 1.0 g, MBA 1.61 mmol L^{-1}, APS 0.5 mmol L^{-1}, 70 ºC, neutralization percent 80%, 60 min).

As reported by other researchers [37], the carboxylate anion interacts with small cations, e.g. Li^+, stronger than with large cations, e.g. K^+. The stronger interactions of carboxylate-small cation have been observed using measurement of activating coefficients of various cations in several salt solutions. As a result, the absorbency in monovalent and divalent cation salt solutions is in the order of $K^+>Na^+>Li^+$ and $Ba^{2+}>Ca^{2+}>Mg^{2+}$, respectively.

Deswelling of Hydrogels in Various Salt Solution

Dewatering kinetic of the swollen hydrogels was measured in different saline solutions which results were represented in Figures 14-17.

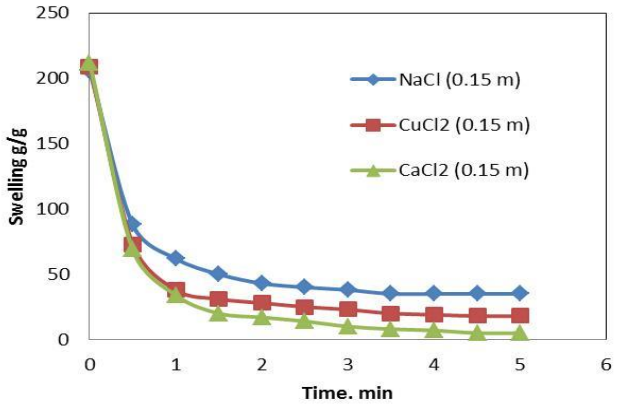

Figure 14. deswelling capacity of the superabsorbent hydrogel nanocomposites in different salt solutions. (Reaction conditions: AAm/ AA 0.186, Na-MMT/gelatin 0.0 g, MBA 1.61 mmol L^{-1}, APS 0.5 mmol L^{-1}, 70 ºC, neutralization percent 80%, 60 min).

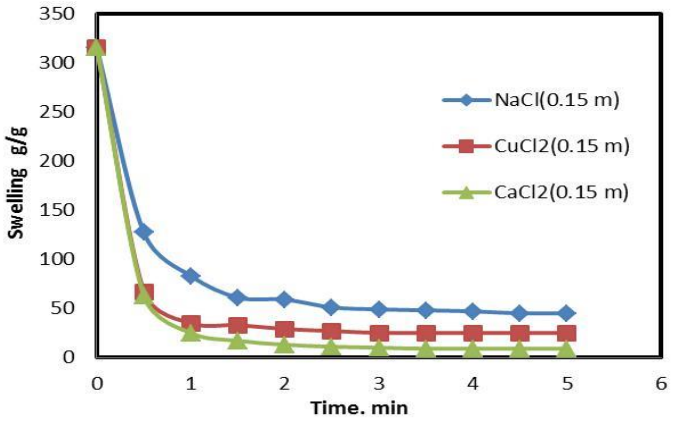

Figure 15. deswelling capacity of the superabsorbent hydrogel nanocomposites in different salt solutions. (Reaction conditions: AAm/ AA 0.186, Na-MMT/gelatin 0.5 g, MBA 1.61 mmol L^{-1}, APS 0.5 mmol L^{-1}, 70 ºC, neutralization percent 80%, 60 min).

As is observed, dewatering rate of samples increases with increasing of the cations charge because crosslinking degree between carboxylate groups and divalent ions is more than monovalent ions. Also Ca^{2+} ions, have a bigger cationic radius than the Cu^{2+} ions; therefore, the degree of crosslinking with functional groups is more than that of the Cu^{2+} ions. According to Figures 14-17, minimum deswelling rate is related to NaCl solution and the maximum deswelling rate is related to $CaCl_2$ solution.

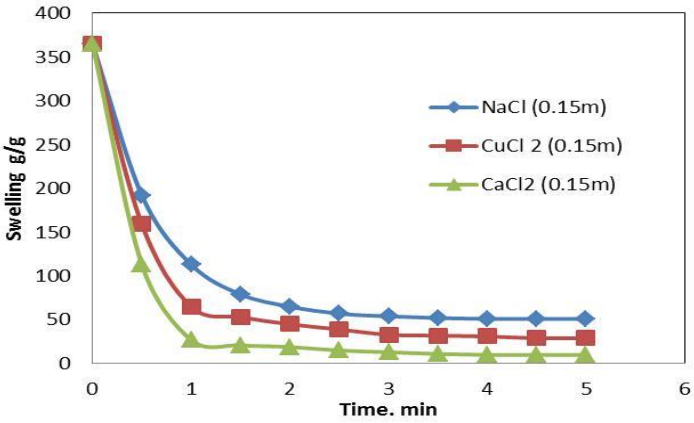

Figure 16. Deswelling capacity of the superabsorbent hydrogel nanocomposites in different salt solutions. (Reaction conditions: AAm/ AA 0.186, Na-MMT/gelatin 0.75 g, MBA 1.61 mmol L^{-1}, APS 0.5 mmol L^{-1}, 70 ºC, neutralization percent 80%, 60 min).

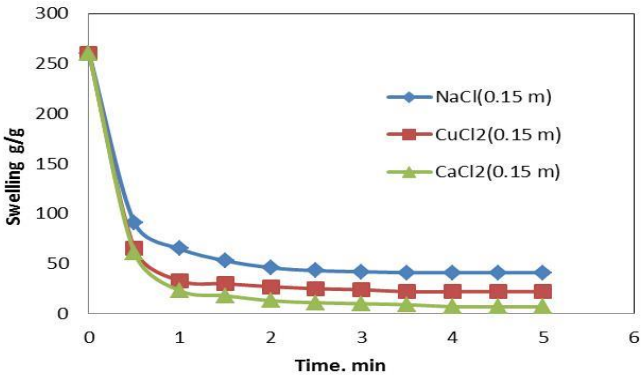

Figure 17. deswelling capacity of the superabsorbent hydrogel nanocomposites in different salt solutions. (Reaction conditions: AAm/ AA 0.186, Na-MMT/gelatin 1.0 g, MBA 1.61 mmol L^{-1}, APS 0.5 mmol L^{-1}, 70 ºC, neutralization percent 80%, 60 min).

Water Retention Capacity (WRC)

One of the significant characteristic of superabsorbents is their water retention capacity because it is very important in some practical usage like agricultural industry. Figure 18 illustrates the water retention capacity of nanocomposites and clay-free superabsorbent at 60 ºC. The existing water in the hydrogels include three kind of water as free water, semi linked and linked water. When the hydrogels exposed to heating, they first lose their free and semi linked water, then the linked water would be lost gently. According to Figure 18, the hydrogel with 0.75 g nanoclay needs more time to lose water than samples with 0.0, 0.5 and 1.0 g nanoclay. Despite more absorption ratio of 0.5 g nanoclay sample (313 g/g) than 1.0 g nanoclay sample (250 g/g), but they lose water almost in same time. This is because of thermal strength effect of composite that cause by nanoclay (Na-MMT).

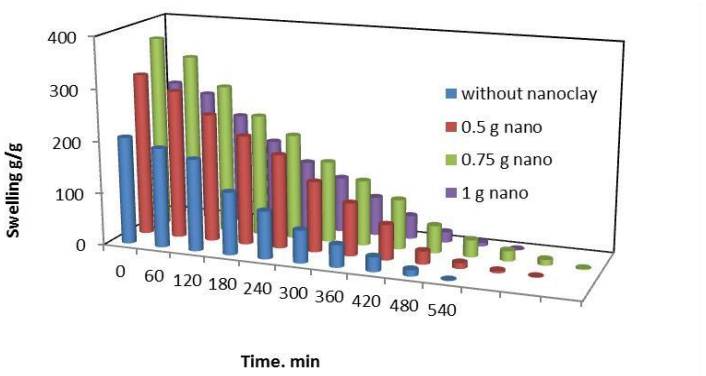

Figure 18. Relationship between heating time and water retention capacity of the hydrogel nanocomposites and the sample without nanoclay at 60ºC.

Conclusion

New hydrogel nanocomposites were synthesized based on protein and AA and AAm comonomers in the presence of nanoclay particles. SEM micrograph of optimized nanocomposite showed an undulant and porous surface without agglomeration. This porosity caused high rate of swelling for the nanocomposite. XRD profile of optimized nanocomposite shows that the clay layers are completely exfoliated and uniformly dispersed in organic matrix. From thermogravimetric curves of the hydrogels was found that the thermal stability of the nanocomposite was clearly improved than the free-clay hydrogel. The best water absorption capacity and gel strength of the hydrogel were observed in the sample containing 0.75 g of Na-MMT. pH-Dependent swelling of the hydrogels was investigated by varying pH of swelling media. From swelling kinetic experiments found that all of the nanocomposites have a higher swelling rate than the pure hydrogel. The hydrogel nanocomposites exhibit good thermal strength, swelling in salt solutions and also deswelling behavior in different saline solutions that can make them useful in agriculture fields.

References

[1] F.L. Buchholz, A.T. Graham, Modern superabsorbent polymer technology. Wiley-VCH, New York (1998).

[2] M.J. Zohuriaan-Mehr, K. Kabiri, *Iran. Polym. J.*, 17, 451 (2008).

[3] T. Inoue, G. Chen, K. Nakamae, A.S. Hoffman, *Polym. Gels Netw.*, 5, 561 (1998).

[4] S.K. De, N.R. Aluru, B. Johnson, W.C. Crone, D.J. Beebe, J. Moore, *J. Microelectromech. Syst.*, 11, 544 (2002).

[5] K. Pagonis, G. Bokias, *Polym. Bull.*, 58, 289 (2007).

[6] Y. Murali Mohan, P.S. Keshava Murthy, K. Mohana Raju, *React. Funct. Polym.*, 63, 11 (2005).

[7] K. Mohana Raju, M. Padmanabha Raju, Y. Murali Mohan, *Polym. Int.*, 52, 768 (2003).

[8] G.R. Mahdavinia, S.B. Mousavi, F. Karimi, G.B. Marandi, H. Garabaghi, S. Shahabvand,

Express Polym. Lett., 3, 279 (2009).

[9] J. Kost, Encyclopedia of controlled drug delivery; Mathiowitz, E., Ed.; Wiley, New York, 1, 445 (1999).

[10] Y. Chen, Y.F. Liu, H.L. Tang, H.M. Tan, *Carbohyd. Polym*., 81, 365 (2010).

[11] A. Pourjavadi, G.R. Mahdavinia, *Turk. J. Chem.*, 30, 595 (2006).

[12] G. Bagheri Marandi, N. Sharifnia, H. Hosseinzadeh, *J. Appl. Polym. Sci.*, 101, 2927 (2006).

[13] G. Bagheri Marandi, G.R. Mahdavinia, S. Ghafary, *J. Appl. Polym. Sci.*, 120, 1170 (2011).

[14] W. Wang, A. Wang, *Carbohyd. Polym*., 77, 891 (2009).

[15] B.D. Kevadiya, G.V. Joshi, H.M. Mody, H.C. Bajaj, *Appl. Clay Sci*., 52, 364 (2011).

[16] G. Bagheri Marandi, Z. Peyvand Kermani, M. Kurdtabar, *Polym. Plast. Tech. Eng*., 52, 310 (2013).

[17] L.A. Goettler, K.Y. Lee, H. Thakkar, *Polym. Rev*., 47, 291 (2007).

[18] E.P. Giannelis, R. Krishnamoorti, E. Manias, *Adv. Polym. Sci*., 138,107 (1999).

[19] J. Jordan, K.I. Jacob, R. Tannenbaum, M.A. Sharaf, I. Jasiuk, *Mater. Sci. Eng. A*, 393, 1 (2005).

[20] J.Y. Lai, *J. Mater. Sci: Mater. Med.*, 21, 1899 (2010).

[21] M. A. Daniele, A. A. Adams, J. Naciri, S. H. North, F. S. Ligler, *Biomaterials*, 35, 1845 (2014).

[22] T. S. Anirudhan, A. M. Mohana, *RSC Adv*., 4, 12109 (2014).

[23] P. R. Reddy, K. Varaprasad, R. Sadiku, K. Ramam, G. V. S. Reddy, K. M. Raju, N. S. Reddy, *J. Inorg. Organomet. Polym*., 23, 1054 (2013).

[24] J.Y. Lai, Y.T. Li, Biomacromole., 11, 1387 (2010).

[25] G. Bagheri Marandi, H. Hosseinzadeh, *Polym. Polym. Compos*., 15, 395 (2007).

[26] F.M. Fernandes, A.I. Ruiz, M. Darder, P. Aranda, E. Ruiz-Hitzky, *J. Nanosci. Nanotechnol*., 9, 221 (2009).

[27] J. Zhang, A. Wang, *React. Funct. Polym*., 67, 737 (2007).

[28] A. Li, J. Zhang, A. Wang, *J. Appl. Polym. Sci.*, 103, 37 (2007).

[29] X. Xia, J. Yih, N.A. D'Souza, Z. Hu, *Polymer*, 44, 3389 (2003).

[30] H. Omidian, S.A. Hashemi, P.G. Sammes, I. Meldrum, *Polymer*, 39, 6697 (1998).

[31] H. Omidian, S.A. Hashemi, P.G. Sammes, I. Meldrum, *Polymer*, 40, 1753 (1999).

[32] A. Pourjavadi, M. Kurdtabar, *Eur. Polym. J.*, 43, 877 (2007).

[33] Y. Luo, H. Peng, J. Wu, J. Sun, Y. Wang, *Eur. Polym. J*., 47, 40 (2011).

[34] A.I. Raafat, *J. Appl. Polym. Sci.*, 118, 2642 (2010).

[35] W.A. Laftah, S. Shahrir Hashim, A.N. Ibrahim, *Polym. Plast. Tech. Eng*., 50, 1475 (2011).

[36] W.F. Lee, R.J. Wu, *J. Appl. Polym. Sci.*, 62, 1099 (1996).

[37] G. Pass, G.O. Philips, D.J. Wedlock, *Macromolecules*, 10, 197 (1977).